J Neurophysiol 113: 2280–2288, 2015.
First published January 21, 2015; doi:10.1152/jn.00390.2014.

Temporal integration at consecutive processing stages in the auditory pathway of the grasshopper

Sarah Wirtssohn[1,2] and Bernhard Ronacher[1,2]

[1]*Behavioural Physiology Group, Department of Biology, Humboldt-Universität zu Berlin, Berlin, Germany; and* [2]*Bernstein Center for Computational Neuroscience Berlin, Berlin, Germany*

Submitted 22 May 2014; accepted in final form 20 January 2015

Wirtssohn S, Ronacher B. Temporal integration at consecutive processing stages in the auditory pathway of the grasshopper. *J Neurophysiol* 113: 2280–2288, 2015. First published January 21, 2015; doi:10.1152/jn.00390.2014.—Temporal integration in the auditory system of locusts was quantified by presenting single clicks and click pairs while performing intracellular recordings. Auditory neurons were studied at three processing stages, which form a feed-forward network in the metathoracic ganglion. Receptor neurons and most first-order interneurons ("local neurons") encode the signal envelope, while second-order interneurons ("ascending neurons") tend to extract more complex, behaviorally relevant sound features. In different neuron types of the auditory pathway we found three response types: no significant temporal integration (some ascending neurons), leaky energy integration (receptor neurons and some local neurons), and facilitatory processes (some local and ascending neurons). The receptor neurons integrated input over very short time windows (<2 ms). Temporal integration on longer time scales was found at subsequent processing stages, indicative of within-neuron computations and network activity. These different strategies, realized at separate processing stages and in parallel neuronal pathways within one processing stage, could enable the grasshopper's auditory system to evaluate longer time windows and thus to implement temporal filters, while at the same time maintaining a high temporal resolution.

temporal integration; facilitation; hearing; leaky energy integration; insects

IN THE AUDITORY SYSTEMS OF various species the detection thresholds for short stimuli decrease with increasing stimulus duration, indicating a temporal integration of sound (Plomp and Bouman 1959; Okanoya and Dooling 1990; Viemeister et al. 1992; Faure and Hoy 2000; Kastelein et al. 2010). These so-called duration/intensity trade-off experiments usually reveal integration time constants of up to several hundred milliseconds. Such large integration time constants, however, seem at odds with the results of other experimental paradigms, such as gap detection and modulation transfer functions, that reveal a high temporal resolution of the auditory system in the range of a few milliseconds. These contradictory observations were referred to as the temporal integration-resolution paradox (de Boer 1985; Green 1985). Remarkably, detection thresholds were also found to be lower when pairs of very short clicks were presented, compared with the presentation of a single click (e.g., Viemeister and Wakefield 1991; Surlykke and Bojesen 1996; Tougaard 1996; see also Heil et al. 2013). Such experiments revealed temporal integration time constants of only a few milliseconds that approach the time constants found, e.g., in the gap detection paradigm. Apparently these experiments reflect different aspects of auditory time constants than those measured in the duration/intensity trade-off experiments.

Psychoacoustic experiments on humans indicated that detection thresholds depend on energy integration, which traditionally have been described by leaky integrator models (e.g., Garner 1947; Plomp and Bouman 1959; Zwislocki 1960). More recent studies, however, suggested that integration of sound pressure rather than of sound energy explains detection thresholds in vertebrate ears, both in cortical neurons and on the perceptual level in mammals (including humans), and in fish and birds (Heil and Neubauer 2001, 2003). Heil and Neubauer (2003) proposed that the integrator is located in the synapse between the inner hair cell and the auditory nerve fiber. They further proposed a solution to the integration-resolution paradox: the decrease in detection threshold with increasing sound duration could be based on an increase in the mean rate of individual subevents (e.g., calcium-binding steps in synaptic processing; for a review, see Heil 2004). As an alternative, a decrease of detection thresholds with stimulus duration has been attributed to the summation of detection probabilities rather than to the integration of sound energy in insect ears (Tougaard 1998).

In insect ears, the auditory receptor neurons were described as energy detectors (Surlykke et al. 1988; Tougaard 1996; Gollisch et al. 2002); the same is suggested for interneurons in the auditory pathway of katydids (Faure and Hoy 2000) and crickets (Sabourin et al. 2008). Gollisch and Herz (2005) described the auditory transduction in the locust ear with an energy integration model, comprising a series of two linear filters and two nonlinear transformations. Anatomical differences in the vertebrate and invertebrate ear may be the cause for the integration of different sound properties: in locusts, the receptors are directly attached to the tympanic membrane, and the receptor axons form the fibers of the auditory nerve (e.g., Michelsen 1971; Römer 1976).

Several studies investigated the temporal resolution capacities of grasshoppers (e.g., Franz and Ronacher 2002; Prinz and Ronacher 2002; Ronacher et al. 2008). Here, we use the grasshopper auditory pathway as a model system to investigate temporal integration at different processing stages. Many grasshopper species rely on acoustic signaling for mate recognition and attraction. Therefore, their auditory system needs to reliably extract song features to recognize conspecifics and to evaluate a potential mate's attractiveness (von Helversen 1972; Stange and Ronacher 2012). The first stages of the grasshopper auditory pathway are located in the metathoracic ganglion and

Address for reprint requests and other correspondence: S. Wirtssohn, Humboldt-Universität zu Berlin, Institute of Biology, Behavioural Physiology Group, Invalidenstraβe 43, 10115 Berlin, Germany (e-mail: sarah.wirtssohn@biologie.hu-berlin.de).

consist of a highly accessible three-layered feed-forward network that is conserved between grasshopper species (Römer and Marquart 1984; Stumpner and Ronacher 1991; Neuhofer et al. 2008). It comprises ~60 receptor neurons per ear that project onto ~15 first-order interneurons, the local neurons, via excitatory synapses; these neurons in turn convey excitatory and inhibitory input onto ~20 second-order interneurons, the ascending neurons (Römer and Marquart 1984; Stumpner and Ronacher 1991; Jacobs et al. 1999; Stumpner and von Helversen 2001; Vogel et al. 2005; Vogel and Ronacher 2007). The ascending neurons transmit the processed information about auditory stimuli to the brain, where the song attractiveness is evaluated and ultimate behavioral decisions are triggered (Ronacher et al. 1986; Bauer and von Helversen 1987).

Auditory receptor neurons faithfully encode the amplitude modulations, i.e., the envelope, of a sensory stimulus in their spike patterns (e.g., Machens et al. 2001; Rokem et al. 2006), whereas the ascending neurons rather respond to specific stimulus features (Stumpner et al. 1991; Ronacher et al. 2004). Recent studies suggest that a change in coding strategy occurs in the auditory pathway, namely from a summed population code with emphasis on the timing of spikes, implemented in the receptors and local neurons, to a labeled-line code implemented in the ascending neurons (Clemens et al. 2011, 2012; see also Hildebrandt 2014). Since ascending neurons exhibit specific auditory filters with different properties, the assumption of a uniform temporal integration time constant in ascending neurons or in the whole auditory system seems less likely. On the other hand, neuron-specific temporal integration properties could enable particularly the ascending neurons to detect (species-specific) features in an amplitude-modulated sound. Different types of temporal integration could thereby form a neurophysiological basis for a labeled-line code in the ascending neurons. Hence, studying temporal integration at consecutive stages in the auditory pathway may help to reveal auditory filters as well as temporal limitations on auditory processing and may give hints to the underlying mechanisms.

We performed intracellular recordings from morphologically identified neurons at three subsequent processing stages in *Locusta migratoria*, while measuring the detection thresholds for single clicks and pairs of clicks with varying interclick intervals (ICIs). In addition, we studied the potential underlying physiological mechanisms by analyzing the postsynaptic potentials of some of these neurons.

MATERIALS AND METHODS

Animals and Electrophysiology

We used male and female locusts (*Locusta migratoria*), obtained from commercial suppliers. Animals were kept at room temperature with ad libitum food supply.

We recorded from morphologically identified neurons in the metathoracic ganglion of the locusts. Detailed procedures on animal preparation, neuron staining and identification are given in Vogel et al. (2005) and Weschke and Ronacher (2008). During recording, the preparation was kept at a constant temperature of 30 ± 2°C by means of a Peltier element. The preparation was placed in a Faraday cage lined with pyramidal foam to minimize echoes.

Electrodes were made from glass borosilicate capillaries (GC100F-10; Harvard Apparatus) by using a horizontal puller (P87 or P-2000, Sutter Instruments) and filled with 3–5% Lucifer Yellow in 0.5 M LiCl. Electrode impedances ranged from ~25 to ~120 MΩ but mostly between 50 and 90 MΩ. Intracellular signals were amplified (SEC05LX; npi electronics) and digitized with an A/D converter (PCI-MIO-16E-4; National Instruments). In parallel, we recorded the envelope of our digital output signal (that is, the acoustic stimulus). Since the click stimuli presented were extremely short with a total duration of 40 μs/click, an unusually high sampling rate of 80 kHz was used. The membrane voltage and the acoustic stimuli were stored via a custom-made program (LabView 7; National Instruments) on a personal computer. Spikes were detected offline by applying a voltage threshold.

Acoustic Stimulation and Stimulus Protocols

Sounds were generated with a custom-made program (Matlab; The MathWorks) on a personal computer. The signals were delivered via a 100-kHz D/A-converter (PCI-MIO-16E-4) and attenuation (ATN-01M; npi electronics) to an amplifier (Mercury 2000; Jensen) that drove a set of speakers (RT-7 Pro; Expolinear). The speakers were placed at a 90° and −90° angle with respect to the longitudinal axis of the preparation, each one at a distance of ~40 cm from one of the animal's ears. Sound intensity was calibrated with a microphone (1/2 in.; type 4133; Brüel & Kjær) and a measuring amplifier (type 2209; Brüel & Kjær). When a stable recording was established, a rate-intensity response curve was measured by presenting 100-ms noise pulses from the left and the right loudspeaker. The pulses were presented in 8-dB steps from 32 to 88 dB and repeated at least three times. The click stimuli were then presented from the more effective side.

We obtained the detection threshold for single clicks and click pairs with varying ICIs. Five repetitions of a single click were presented in 8-dB steps from 32- to 88-dB SPL to get a rough first estimate of the detection threshold. The rough first threshold estimate was evaluated online by visually monitoring poststimulus spiking activity in the membrane voltage trace displayed on an oscilloscope. Thus we could roughly determine the intensity range of interest. For finer estimation of the detection threshold, we then presented single clicks (5 or 10 repetitions) and click pairs with varying ICIs (10 repetitions each), in 2-dB steps around the rough threshold estimate, usually covering a range of 10–16 dB. The ICIs tested were 1, 2, 3, 4, 6, 8, 10, 20, and 30 ms. Figure 1*A* shows the digital single and click pair waveforms used to drive the loudspeakers and microphone recordings of the air pressure fluctuations at the site of the animal's ear.

Data Analysis

All data analysis was carried out using Matlab (The MathWorks), except for linear regression fits to first-spike latencies which were calculated in Excel 2013 (Microsoft Office).

Because neurons commonly responded with one spike to a click near threshold, neurons with high rates of spontaneous activity had to be excluded from further analysis. We analyzed the following cells: 8 receptors, 17 local neurons, and 15 ascending neurons (ANs). It was not determined whether the receptor neurons were of the high- or low-frequency type (compare, e.g., Michelsen 1971). The local neurons can be divided into primary-like local neurons (TN1, $n = 8$; SN1, $n = 1$) and nonprimary-like local neurons (BSN1, $n = 7$). Ascending neurons can be grouped into direction-coding neurons (AN1, $n = 7$; AN2, $n = 2$) and pattern-coding neurons (AN11, $n = 2$; AN12, $n = 3$); these ascending neurons are all excited by auditory input. The AN10 neuron plays a role in sensorimotor integration and is excited by auditory input (e.g., Pearson et al. 1985). Since not each single cell was tested with every ICI, the exact n for different cell types for each stimulus is given in the RESULTS.

Determination of detection thresholds. To assess the integration time of the neurons, the detection threshold for the single clicks and click pairs had to be defined. To this end, for each individual neuron the poststimulus time histogram for each stimulus across all intensities was visually inspected. A time window (ranging 5–60 ms after stimulus onset) with stimulus-related activity could thus be chosen,

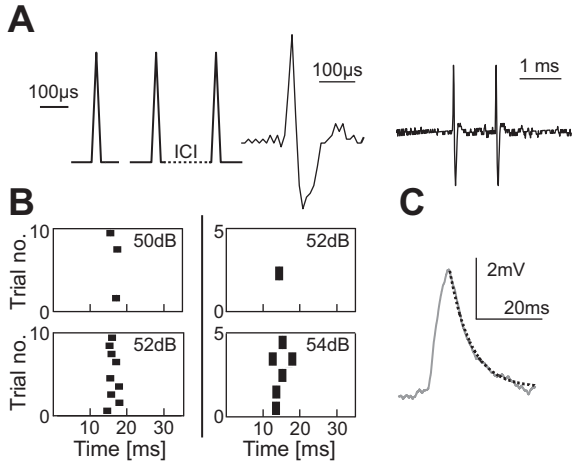

Fig. 1. *A*, *left*: triangular single and click pair waveforms used to drive the loudspeakers. Each click had a total duration of 40 μs. The interclick interval (ICI) between the click pairs was systematically varied. *Middle* and *right*: air pressure fluctuations evoked by a single click and by click pairs with a 1-ms ICI, measured at the site of the animal's ear with a high precision microphone. *B*, *left*: spike raster plot of a neuron with 10 single click repetitions. Detection threshold determined with sign test ($P < 0.05$) to be 52 dB; the stimulus is subthreshold at lower intensities, here at 50 dB. *Right*: spike raster plot of a neuron with 5 single click repetitions. The detection threshold is 54 dB, based on the criterion that the neuron responded in at least 80% of the trials. At 52 dB the click is subthreshold. Stimulus onset at 0 ms. *C:* excitatory postsynaptic potential (EPSP; grey line) and exponential fit (dotted black line) to parametrize EPSP decay time constant.

such that the activity of the neuron was evaluated during the identical time window at all intensities. The spontaneous activity of the neuron was determined in a time window of the same length before stimulus onset. A sign test was conducted to compare the spike count during spontaneous activity and the spike count during the time window where stimulus-induced activity was expected. Separate tests were performed for each stimulus and at each intensity. The lowest intensity at which poststimulus activity significantly exceeded spontaneous activity ($P < 0.05$) was considered the detection threshold of the neuron for the specific stimulus (Fig. 1*B*, *left*).

In some recordings we presented only five stimulus repetitions of the single click and thus the sign test could not be used to calculate the detection threshold. Because neurons commonly responded with only one spike per click to stimuli near the threshold, any spike false positively counted as a "detection" of the stimulus will strongly affect the results. Therefore, it was ensured that in these specific recordings no spontaneous spikes occurred during 130 ms before stimulus onset. Since the neurons thus showed a negligible spontaneous firing activity, we considered it unlikely that spikes occurred spontaneously in the short time window after stimulus presentation. These neurons were therefore included into further analysis and the detection threshold was determined as the lowest intensity at which the neuron responded with at least one spike to the stimulus in at least 80% of the trials (Fig. 1*B*, *right*). This procedure was applied to four individual neurons (2 TN1 and 2 BSN1).

After the detection threshold for each specific stimulus was calculated, that is, single clicks and click pairs with varying ICIs, the data were pooled by neuron type. To this end we calculated the difference between the detection thresholds for click pairs, Thresh_{cp}, and the detection threshold for single clicks, Thresh_{sc}, which gave us a single measure of the relative threshold difference, Δthreshold, for each neuron. Hence, Δthreshold is given by

$$\Delta\text{threshold} = \text{Tresh}_{cp} - \text{Tresh}_{sc}.$$

Negative values of Δthreshold thus indicate a lower detection threshold for click pairs. This evaluation allowed us to plot the calculated Δthreshold values as a function of the click pair ICIs for each neuron type, and we inferred the degree and time courses of temporal integration from these data plots.

As mentioned above, temporal integration is often described by leaky energy integration (e.g., Plomp and Bouman 1959; Zwislocki et al. 1960, 1962). Therefore, we tested this model by fitting an exponential function to part of the data with the least-squares method. Accordingly, Δthreshold is described as a function of the ICI of the click pair (Δt) by

$$\Delta\text{threshold} = -10\log\left(e^{\frac{-\Delta t}{\tau}} + 1\right),$$

where τ is the time constant of the leaky integrator (see also Tougaard 1996). Note that τ here corresponds to the time point when the effect is reduced by 50%, that is, Δthreshold reaches half of its maximal absolute value.

Analysis of postsynaptic potentials. To assess possible underlying neurophysiological mechanisms of temporal integration, we studied the excitatory postsynaptic potentials (EPSPs) in dendritic recordings of single specimens of BSN1 and AN12. To accomplish this, the membrane voltage traces in subthreshold stimulus trials (that is, trials in which the stimulus was presented at intensities below detection threshold and no spike occurred after the stimulus) were smoothed with a moving average window of 0.0625 ms and averaged. The inclusion criterion was at least eight subthreshold stimulus trials without a spike response. The baseline activity of the neuron was calculated as the mean potential during the 130 ms before stimulus onset. If spontaneous spikes occurred, they were excluded so as to not influence baseline measures. The standard deviation of the baseline activity was calculated as the standard deviation during the same time window. An EPSP was considered to have occurred when the amplitude of the potential after stimulus onset increased to a value $>$ baseline potential $+ 3 \times$ standard deviation.

EPSP amplitudes were determined as the difference between the baseline voltage and the maximum voltage peak. Exponential functions were fitted to the decaying phase of the EPSP, or to the decaying phase after the last peak in a compound EPSP, to determine the decay time constant (Fig. 1*C*). To quantify the duration of the excited state, we further calculated full duration at half-maximum values (FDHM).

Note, however, that the EPSP analysis has some limitations, particularly since dendritic recordings were available only for single specimens; in addition the EPSP shapes could only be correlated to the stimuli, and the influence of passive membrane capacities could not be disentangled from presynaptic processes. However, finding EPSPs as a response to a subthreshold stimulus shows that these definitely occur in a specific neuron type. Therefore, our results should be regarded as examples of possible integration mechanisms and their time courses, clearly showing that temporal integration is not purely presynaptic to specific neuron types but can be based on neuron-intrinsic computations in higher order neurons.

RESULTS

The time courses of the detection threshold shifts revealed a number of different mechanisms of temporal integration implemented in the locust auditory pathway. As a criterion for leaky integration, the detection threshold should monotonically increase with increasing stimulus intervals. Energy integration can only yield a maximal threshold shift of -3 dB, since a doubling of sound energy corresponds to a $+3$ dB higher sound intensity. With those criteria the leaky energy integration model was only applicable to the auditory receptor neurons and the primary-like local neurons (TN1 and SN1). Higher order neurons showed mainly two distinct phenomena: either, no temporal integration effects on threshold, or strong nonmonotonic threshold shifts with a range of "optimal" ICIs.

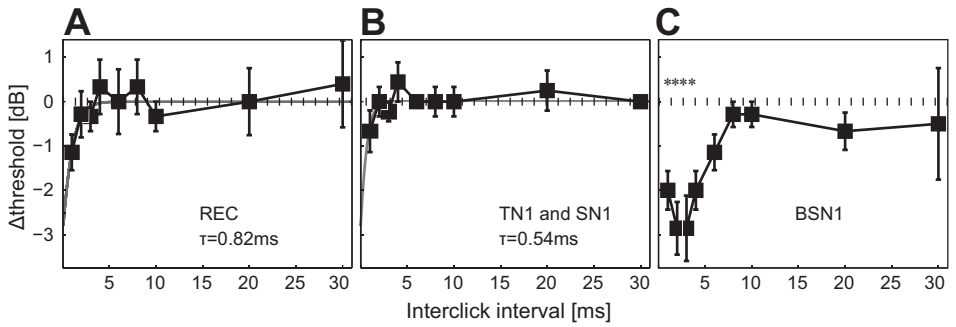

Fig. 2. Temporal integration in receptor neurons and local neurons. At Δthreshold = 0 (grey stippled lines), the detection thresholds for the click pairs were the same as for a single click. *A*: temporal integration in receptor neurons ($n = 8$; 2- and 20-ms ICIs, $n = 7$; 3-, 4-, and 8-ms ICIs, $n = 6$; 10- and 30-ms ICIs, $n = 5$) could be described with a leaky energy integrator model with a time constant of 0.82 ms (grey curve, $R^2 = 0.69$). *B*: temporal integration in primary-like local neurons (TN1 and SN1) ($n = 9$; 8-, 10-, and 20-ms ICIs, $n = 8$; 30-ms ICI, $n = 1$) was close to the findings in receptor neurons. The leaky integrator model could be fitted with a time constant of 0.54 ms (grey curve, $R^2 = 0.58$). *C*: temporal integration in the nonprimary-like local neuron BSN1 ($n = 7$; 30 ms, $n = 4$). At 1- to 4-ms ICIs the threshold reduction was significant ($P < 0.05$, Wilcoxon signed rank-test). *A–C*: values are means, and error bars depict SE.

Leaky Energy Integration

Figure 2*A* shows the differences between the thresholds found for a single click and for click pairs with increasing ICIs for the receptor neurons. A clear threshold reduction occurred at an ICI of 1 ms, whereas at larger click separations the two-click paradigm resulted in similar thresholds as a single click (Δthreshold = ~0). The results were consistent with energy integration by a leaky integrator with a time constant of 0.82 ms (Fig. 2*A*; $R^2 = 0.69$). The same effect was found for the primary-like interneurons TN1 and SN1 (Fig. 2*B*); the detection threshold reduction resembled that of receptors, but the effect was weaker. A leaky energy integrator model could be fitted with a time constant of 0.54 ms ($R^2 = 0.58$). However, the time constant estimates in both the receptors and primary-like local neurons are probably still too large, in view of the fact that the smallest ICI used was 1 ms. In any case, it is clear that the integration time constant was <1 ms, and the primary-like local neurons did not exhibit any indication of temporal integration that exceeded the effect found in receptor neurons.

No Clear Indication of Temporal Integration

Two types of ascending neurons (AN2 and AN11; Fig. 3, *A* and *B*) showed no clear indication of temporal integration. These findings are puzzling, since we found temporal integration in the receptors; accordingly, higher order interneurons should at least show the same threshold shift at a 1-ms ICI as the receptors. This issue will be addressed later in the DISCUSSION.

Temporal Integration at Specific ICIs in Higher Order Interneurons

Other neurons displayed strong threshold shifts, with maximal reduction at specific ICIs. This group comprises four neuron types: the local neuron BSN1 and the ascending neurons AN1, AN10, and AN12.

As can be inferred from Fig. 2*C*, the BSN1 exhibited a clear threshold reduction up to a 6-ms ICI; this effect was significant at 1- to 4-ms ICIs ($P < 0.05$, Wilcoxon signed rank test). A larger reduction in threshold occurred at 2- to 3-ms ICIs than at a 1-ms ICI. On the single neuron level, four out of seven neurons had a lower threshold at 2 and/or 3 ms than at a 1-ms ICI; and in no specimen was the 1-ms threshold below the threshold at 2- and/or 3-ms ICIs. In the AN1 neurons we found a maximal threshold shift of −3 to −4 dB (Fig. 3*C*). The effect was strongest at 3- to 6-ms ICIs (significant with $P < 0.05$, Wilcoxon signed rank test). In four out of seven specimens, the threshold was lowest at ICIs between 3 and 6 ms, and in none of the neurons was the threshold higher at 3- to 6-ms ICIs than at 1- and/or 2-ms ICIs. The threshold reduction extended up to 8 ms. In a third group of neurons (AN10 and AN12), the effect of click pairs on detection threshold was even stronger, with threshold shifts of −6 dB and ~−7 dB, respectively, for click pairs (Fig. 3, *D* and *E*). Again, the threshold did not increase monotonically

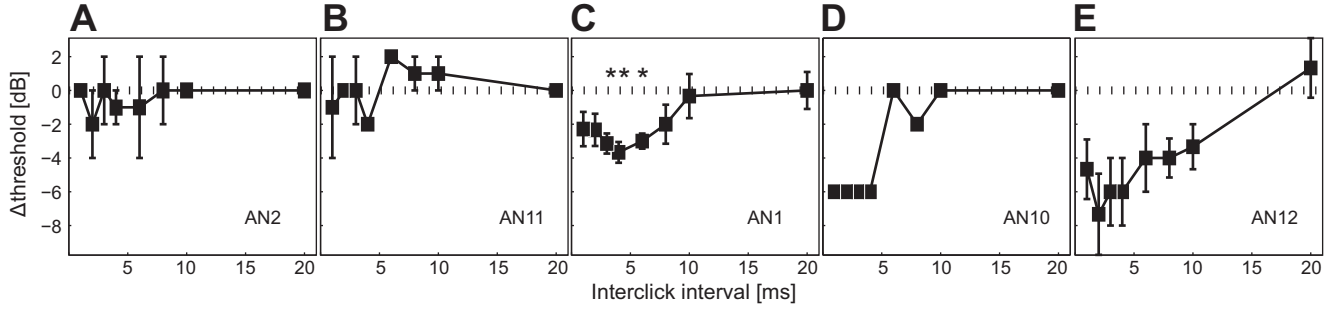

Fig. 3. Detection thresholds in ascending neurons. At Δthreshold = 0 (grey stippled lines) the click pair thresholds were the same as for the single click. *A* and *B*: in ascending neurons AN2 ($n = 2$) and AN11 ($n = 2$), the threshold for click pairs was not systematically lower or higher than for single clicks. *C*: in AN1 ($n = 7$; 2- and 4- to 10-ms ICIs $n = 6$; 20-ms ICI, $n = 5$) a threshold reduction for click pairs occurred, with lowest thresholds at 3- to 6-ms ICIs (significant with $P < 0.05$, Wilcoxon signed rank-test). *D* and *E*: in AN10 ($n = 1$) and AN12 ($n = 3$), strong threshold reductions occurred. *A–E*: values are means, error bars depict SE.

with ICI, but occurred at an optimal time window: at ICIs ≤4 ms in AN10 and 2- to 4-ms ICIs in AN12. In AN12, the detection thresholds at 2- to 4-ms ICIs were at least as low as at a 1-ms ICI in all neurons and lower in two out of three neurons. The threshold reduction was still visible at a 10-ms ICI.

Due to the nonmonotonic shape of the temporal integration curves, a leaky integration model could be excluded for the local neuron BSN1 and the ascending neurons AN1, AN10, and AN12. Theoretically, in a click pair-paradigm two mechanisms could lead to the reduction in detection threshold determined by a spike count measure, as applied in this study. First, due to a "joint probability" effect: when a close-to-threshold event (as a single click) occurs, it is detected with a certain probability. If the detection probability was independent for each click in a pair and no integration occurred, these detection probabilities for each event would sum up (see Tougaard 1996, 1998). Second, the two clicks of a click pair could be temporally integrated. To test how strongly our results are influenced by "joint probability," we analyzed first spike latencies. If the first-spike latencies are latency locked to the ICI duration, this indicates a temporal integration effect. Most spikes clearly occurred after the second click in BSN1, AN1, AN10, and AN12 (Fig. 4), and the latencies increased systematically with ICI. The influence of joint probability was low since only few singular spikes occurred as a response to the subthreshold first click of the pair. Thus the threshold shifts observed were not artifacts of joint probability but were based on temporal integration.

While a subpopulation of ANs did not show any consistent effects of temporal integration, other ANs and the local neuron BSN1 showed nonmonotonic threshold shifts with maximal threshold reductions at neuron-specific "optimal" ICI windows. How do these different effects arise: are they based on presynaptic network activity or on neuron-intrinsic computations? We will now investigate possible underlying mechanisms by looking at the shapes of postsynaptic potentials in BSN1 and AN12.

Postsynaptic Potentials Underlying Temporal Integration

One possible way to distinguish neuron-intrinsic and presynaptic network computations in intracellular recordings is to correlate the time courses of postsynaptic potentials with the stimulus. To this end, we looked at EPSPs evoked by the acoustic stimulation in a dendritic recording from BSN1 and AN12.

In BSN1 a clear EPSP was elicited by a single click presented with subthreshold intensity starting from 4 dB below single click threshold (Fig. 5*A*). EPSP amplitudes were significantly larger at higher sound pressure levels (4 dB below threshold vs. 2 dB below threshold; $P < 0.05$, Kruskal-Wallis-test). There was no clear relationship found between ICI and EPSP amplitude. Decay time constants of the subthreshold EPSPs were not significantly different for increasing sound pressure levels or across ICIs (mean decay time constant: 4.2 ± 1.5 ms). A linear relationship ($R^2 = 0.86$ and 0.89, respectively) was found when looking at the EPSP FDHM, which increased with increasing ICI but only up to a 4-ms ICI (Fig. 5*C*); this increase in FDHM was based on temporal summation of the excitatory synaptic inputs for short ICIs (Fig. 5*B*). Note that this is also the range in which the detection threshold shift was most prominent. From an ICI of ≥6 ms on, the EPSP shape showed two distinct peaks such that the first peak had a FDHM value comparable to that elicited by a single click (mean: 5.67 ± 1.6 ms for click pairs with ICI ≥6 ms, 5.73 ± 0.36 ms for a single click). That is, no substantial integration of the second click occurred at the level of the EPSP in the BSN1 at ICIs ≥6 ms, which is consistent with the time range of the temporal integration on the BSN1 group level (Fig. 2*C*).

AN12 exhibited a clear EPSP as a response to single clicks presented at subthreshold intensities, starting at least 8 dB below detection threshold (which was the lowest intensity presented during this recording); see Fig. *5D* for single trial EPSPs evoked by a single click at different intensities. The shapes of the single trial EPSPs reveal that the underlying mechanism for integration in the AN12 was neuron-intrinsic temporal summation (Fig. 5*E*). However, at 1- to 4-ms ICIs, the first EPSP peak was much larger than at longer ICIs; this implies that at small ICIs, the neuron may receive already integrated input from the presynaptic network. The FDHM of the EPSP increased fairly linearly between 4- and 10-ms ICIs ($R^2 = 0.45–0.99$, Fig. *5F*), roughly corresponding to the range of temporal integration in Fig. 3*E*. The time constants for the

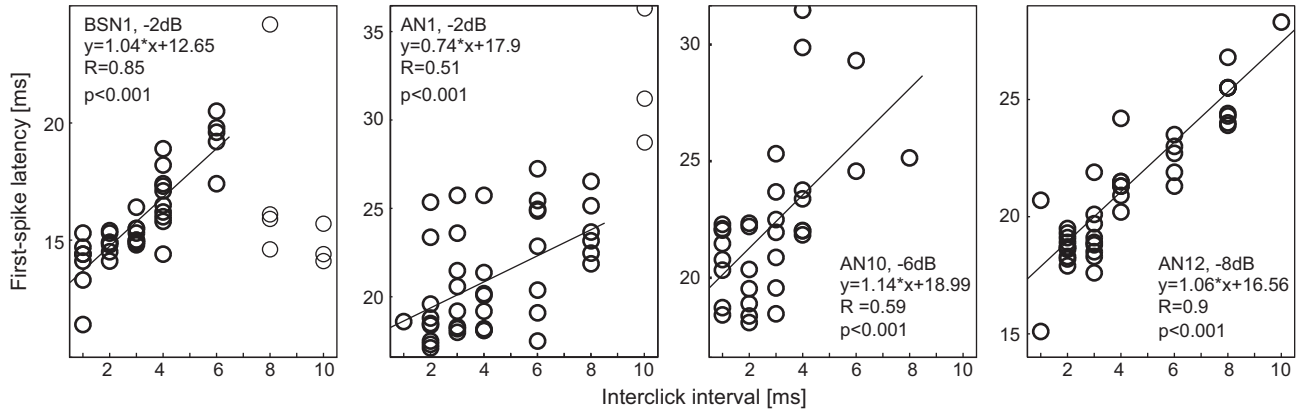

Fig. 4. First spike latencies to click pair stimuli of typical single neurons, stimulated at intensities below single click detection threshold. Linear regression lines were fit to the 1st-spike latencies at all ICIs in which a threshold shift occurred at the group level in the neuron type (data points printed in bold): 1- to 6-ms ICIs in BSN1, 1- to 8-ms ICIs in AN1, 1- and 8-ms ICIs in AN10, and 1- and 10-ms ICIs in AN12 (compare Fig. 2*C* and Fig 3*C-E*). The 95% confidence interval of the regression fits enclose the value 1, though in AN1 the slope was <1. A slope close to 1 indicates a linear increase of the 1st spike latency with the timing of the 2nd click and thus a response integration or facilitation.

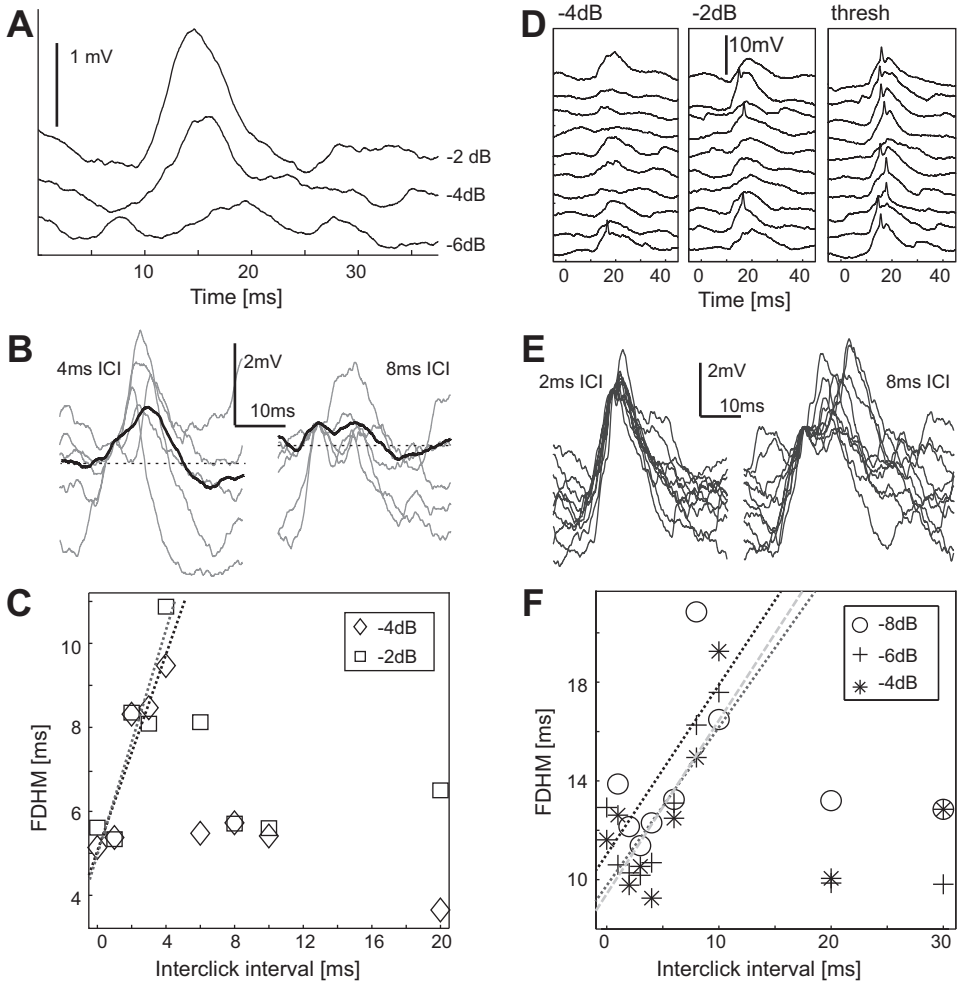

Fig. 5. Analysis of postsynaptic potentials in BSN1 (*A–C*) and AN12 (*D–F*). *A:* membrane potential of BSN1 after a single click, −6 dB (trials averaged $n = 10$), −4 dB ($n = 8$), and −2 dB ($n = 8$) relative to detection threshold. A single click elicits a clear EPSP starting from −4 dB. *B:* mean EPSP (black) evoked by a click pair stimulus with a 4-ms ICI (trials averaged $n = 9$) and 8-ms ICI ($n = 9$), 4 dB below single click detection threshold. Black stippled lines: baseline value before stimulus onset. Grey: example single trial traces. All EPSPs are aligned to the 1st peak. The 2nd peak of the EPSP was higher than the 1st peak in single all trials at a 4-ms ICI but at a 8-ms ICI in only 4 out of 9 trials. *C:* full-duration-at-half-maximum (FDHM) of EPSP values increase linearly up to an ICI of 4 ms (grey dotted line −2 dB, and black dotted line −4 dB below single click threshold), at ICIs ≥6 ms the FDHM drops back to durations as elicited by a single click (at ICI 0 ms). *D:* single trial EPSPs in the AN12 neuron. Ten single click repetitions presented at −4 dB relative to detection threshold, *left*, at −2 dB, *middle*, and at detection threshold intensity, *right*. *E*: single trial EPSP shapes ($n = 10$), aligned to the 1st peak, indicate that 2nd peak in the EPSP tends to be higher in amplitude at short (here: 2 ms) and longer (here: 10 ms) ICIs. Intensity shown −6 dB relative to single click detection threshold. *F*: FDHM of EPSPs increases in response to click pairs between 4- and 10-ms ICIs for −8, −6, and −4 dB relative to single click threshold. Lines are linear regression lines (black dotted line: −8 dB; grey dotted line: −6 dB; grey stippled line: −4 dB).

EPSP decay for the various stimuli were not significantly different (mean 9.7 ± 1.9 ms). The EPSP amplitudes were significantly larger at 4 dB than at 6 and 8 dB below single click detection threshold ($P < 0.001$, Kruskal-Wallis-test).

Unfortunately, the amplitude of an EPSP cannot be compared across recordings, for instance, to estimate input strength onto BSN1 and AN12, since it depends strongly on the recording site.

DISCUSSION

A major finding of this study is the diversity of response types in different neurons. We found evidence for leaky energy integration in the receptor neurons, with a time constant of 0.82 ms. Primary-like local interneurons did not show effects of temporal integration exceeding those in the receptors. A leaky energy integrator model with a similar time constant could describe the data, and no effects beyond a 1-ms ICI were found. A subpopulation of ANs did not show any consistent effects of temporal integration, whereas some local neurons and ANs showed nonmonotonic threshold shifts with maximal threshold reductions at neuron-specific "optimal" ICI windows.

Leaky Energy Integration at the First Stages in the Locust's Auditory Pathway

Only neurons at the very periphery of the locust auditory pathway, the auditory receptors and the primary-like local neurons, responded in a way consistent with a leaky energy integrator model. The very short time constant in the receptor neurons (probably smaller than 0.82 ms) is in line with results of Gollisch and Herz (2005) on locusts but clearly smaller than the 3.4 and 4.1 ms obtained with a click pair paradigm for the A1 receptors in moths (Tougaard 1996). According to Gollisch and Herz (2005), integration at an ICI of 1 ms is based on electrical integration at the neural membrane, since mechanic integration at the tympanum occurs and decays faster. Windmill et al. (2008) investigated tympanal mechanics with short (15 μs) sound pulses and found that the oscillation of the tympanic membrane outlasted their stimulus by a factor of 10 (see also Schiolten et al. 1981). Hence, even at the smallest ICI used in our study (1 ms), the oscillation of the tympanic membrane elicited with the 40-μs clicks most probably had ceased before the second click reached the tympanum. We conclude that temporal integration at the timescales measured in our experiment is based on neural integration, i.e., accumulation of electrical charges over the neuron's membranes.

Temporal integration in primary-like local neurons (TN1 and SN1) was weak and in the range of temporal integration in the receptors, with a time constant of ~0.5 ms. Apparently, these local neurons did not perform neuron-intrinsic summation of subthreshold input, since the effects found here did not exceed those of the receptor neurons. The short time constants in locust receptor cells and primary-like neurons enable a

precise coding and a high temporal resolution for the analysis of sound signals.

Temporal Integration at Later Processing Stages

The threshold shifts indicative of temporal integration in the ascending and some local neurons (BSN1, AN1, AN10, and AN12) did exceed by far the time constants and shift amplitudes found in receptor neurons and primary-like local neurons. Thus we must postulate additional mechanisms. Maximal threshold reductions occurred at neuron type-specific ICI windows (2–3 ms for BSN1, 3–6 ms for AN1, <6 ms for AN10, and 2–4 ms for AN12). Also, the amplitudes of the maximal threshold reduction differed between neuron types (~−3 dB for BSN1 and AN1, ~−6 dB for AN10, and ~7 dB for AN12).

All higher order interneurons receive their input ultimately from the receptor neurons, either directly via monosynaptic connections or indirectly via synaptic processing of receptor-driven interneurons (e.g., Boyan 1992). The first location where integration effects exceeding the temporal integration in receptor neurons can be produced are the synapses between receptors and the respective local neurons. Various effects could contribute: *1*) the processing within synapses can be highly nonlinear, as is known from many studies investigating, e.g., spike-timing-dependent plasticity and synaptic facilitation and depression (Baker and Carlson 2014; for reviews, see Zucker and Regehr 2002; Dan and Poo 2004). ICI-dependent efficacy of synaptic transmission could therefore affect the integration time course in the postsynaptic cell. *2*) Temporal jitter in presynaptic inputs could further influence integration time in a higher order neuron, for instance, caused by differences in axonal conductance speed (Römer 1976). *3*) Other mechanisms contributing to temporal integration could be active dendritic postsynaptic currents (Remme and Rinzel 2011) or passive membrane properties of the postsynaptic cell, and *4*) different time courses of excitatory and inhibitory input (Stumpner and Ronacher 1991; Oswald et al. 2006). Thus several mechanisms may interact in a complex manner to produce the final temporal integration time window of a higher order neuron. Some mechanisms can be regarded as purely presynaptic to the respective neuron. Others necessarily require neuron-intrinsic computations on top of presynaptic processing, such as the summation of postsynaptic input. Due to this complexity it is difficult to separate the influence of different mechanisms on the temporal integration capabilities of a higher order neuron. Nonetheless, we will try to disentangle at least to some degree presynaptic from neuron-intrinsic effects.

The BSN1 neuron receives input from different receptor populations (Römer and Marquart 1984). Thus the width of its EPSP could be influenced by a temporal jitter of the input delivered by the receptor neurons and by different spike propagation speeds in different receptor populations (Römer 1976; Halex et al. 1988). BSN1 projects onto AN1 (Marquart 1985; Boyan 1992) and could thus mediate temporal integration in the range of its own time constant. The amount of threshold reduction is similar in both neurons. However, as the optimal ICI window is larger in AN1, additional effects seem to contribute to the temporal integration properties of AN1.

A candidate mechanism to explain the finding of "optimal" ICIs for several ANs is neuronal facilitation. Two-tone facilitation has been described for subthreshold stimuli e.g., in the cochlear nerve of gerbils (Henry 1991) and in the cochlear nucleus of guinea pigs (Jiang et al. 1996), visible by a decrease in detection threshold for two consecutive tones. Possible mechanisms for facilitation include the increase of transmitter release probability from residual Ca^{2+} levels in presynapses upon arrival of a second action potential with a brief delay (see Fortune and Rose 2001 for a review on temporal filtering by means of short-term synaptic plasticity). An exclusive tuning to specific ICIs, comparable, e.g., to duration tuning known from the vertebrate midbrain and cortex (e.g., Ehrlich et al. 1997; He et al. 1997), however, was not found in locusts' neurons: all cells in the present study responded to a single click, provided that it was loud enough. A multiple-looks model (Viemeister and Wakefield 1991) can be excluded for this processing stage in the grasshopper, since it incorporates a long-term decrease in detection thresholds in the range of several hundred milliseconds.

Why Do Some Cells Not Exhibit Temporal Integration?

Some cells did not show effects of temporal integration exceeding the integration in receptors, such as the primary-like local neurons TN1 and SN1, others showed no threshold shifts at all (AN2 and AN11). This latter observation was unexpected: since the receptors integrate over short ICIs, at least this effect should be transmitted to later stages. A possible reason for the (apparent) loss of threshold reduction might be that the threshold reduction was rather small in the receptors and primary-like neurons. Thus the increasing variability at the next processing level (see Vogel et al. 2005) might have masked this small effect in a way that it could not be determined in these neurons with the 2-dB steps applied here. However, a so small effect may not be biologically relevant.

Relations Between Temporal Integration and Temporal Filtering?

The very short integration times of receptors and primary-like neurons TN1/SN1 are in line with results obtained in a modulation-transfer-function (temporal MTF) paradigm, where these neurons exhibited high temporal resolution (mean corner frequencies 172 ± 17 Hz, $n = 11$, and 142 ± 43 Hz, $n = 11$, respectively, data from Wohlgemuth et al. 2011 and Weschke and Ronacher 2008). Likewise, the best modulation frequencies (BMFs) were high (131 ± 28 Hz; 103 ± 33 Hz). In ANs corner frequencies and BMFs were distinctly lower: mean corner frequencies of AN1, AN2, and AN12 were found between 40 and 53 Hz ($n = 5, 2, 2$), and of AN11 78 ± 46 Hz ($n = 4$); mean BMFs were uniformly distributed between 30 and 56 Hz (see also Fig. 11.4 in Ronacher 2014). These data of ANs would fit to a more integrative filter type, which leads to lower corner frequencies and lower BMFs (cf. Nagel and Doupe 2006). BSN1 had a somewhat intermediate position between the primary-like local and the ANs (corner frequency: 129 ± 45 Hz; BMF: 81 ± 41 Hz; $n = 15$). However, these results give no hints to explain the differences we observed between AN2 and AN11 on one side, showing no consistent temporal integration (Fig. 3, *A* and *B*), and AN1 and AN12 that showed long-lasting integration effects (Fig. 3, *C* and *E*); AN10 was not included in the earlier sample.

In a modeling study Clemens et al. (2012) found two distinct classes of neurons, largely corresponding to the classes of local neurons and ANs: TN1 and SN1 belonged to the class of

"derivative-like" neurons, whereas BSN1 (phasic subtype), AN1, and AN2 belong to the "leading-suppressive" class. Remarkably, the neurons showed only small differences in the filters derived from the spike-triggered averages (STA filters) but differed mainly in their spike-triggered covariance-filters (Clemens et al. 2012). Unfortunately, their sample did not cover AN11 and AN12, but again the data by Clemens et al. (2012) offer no explanation for the differences between AN1 and AN2 visible in Fig. 3, *A* and *C*. A possible conclusion is that the cellular processes investigated with the click pair paradigm bear no direct relation to the phenomena measured in the other paradigms because of the different intensities used. Nagel and Doupe (2006) report strong effects of stimulus intensity on the filter shapes. Hence, a crucial difference may have been the stimulus level, which was 10–15 dB above the respective neuron's threshold in the study of Clemens et al. (2012); similarly, the MTFs were obtained at ~20 dB above threshold (Wohlgemuth et al. 2011). In particular, with sound levels around threshold we found no indications for an inhibitory input to the investigated neurons, whereas interactions between excitation and inhibition, and their respective timing, have been postulated as crucial factors that determine the shape of auditory filters (Clemens et al. 2012; Hennig et al. 2014; Ronacher et al. 2015).

Relation to Long-Term Integration

For the auditory periphery of vertebrates it has been proposed that only short-term integration occurs, and (what seems to be) long-term integration is based on the accumulation of independent synaptic subevents eventually leading to spike generation in an auditory receptor with a time delay; according to this idea, this time delay has been traditionally (mis-)interpreted as long-term temporal integration (Heil and Neubauer 2001, 2003). Other authors have also refuted the idea of long integration time constants in the auditory periphery and argue instead that long-term temporal integration is centrally generated (e.g., Viemeister and Wakefield 1991; Viemeister et al. 1992; Lütkenhöner 2011; Saija et al. 2014). Also, for insects, Tougaard (1998) proposes a distinction between two temporal integration time constants: an intrinsic one, for the peripheral auditory neurons, and a behavioral time constant, generated in the central nervous system. Previous experiments have in fact shown that grasshoppers have "behavioral time constants," substantially longer than the neuronal ones we present here: male grasshoppers (*Chorthippus biguttulus*), for instance, respond to female songs lasting only 250 ms as precisely as to songs of the natural duration of 1,000 ms (Ronacher and Krahe 1998, 2000), which suggests an upper limit for a behavioral integration time constant of ~250 ms.

To summarize, in the locusts' auditory pathway temporal integration properties differ remarkably between neuron types. Only the responses of neurons at the very periphery could be described by a leaky integrator model. In contrast, several neurons at the next processing stages exhibited a stronger threshold reduction at longer ICIs than at the 1-ms interval. We found no clear relation between neuron-specific temporal integration and temporal filters as described by Clemens et al. (2012). The specific mechanisms contributing to these observations must be addressed in future studies.

ACKNOWLEDGMENTS

We thank Matthias Hennig and Jan-Hendrik Schleimer for inspiring discussions, Florian Rau for technical assistance, Michael Reichert and Jan Clemens for helpful comments on the manuscript, and Regina Lübke for animal care.

GRANTS

This work was funded by the German Federal Ministry of Education and Research (BMBF; Grant FKZ 01GQ1001A to B. Ronacher).

DISCLOSURES

No conflicts of interest, financial or otherwise, are declared by the author(s).

AUTHOR CONTRIBUTIONS

Author contributions: S.W. and B.R. conception and design of research; S.W. performed experiments; S.W. analyzed data; S.W. and B.R. interpreted results of experiments; S.W. prepared figures; S.W. drafted manuscript; S.W. and B.R. edited and revised manuscript; S.W. and B.R. approved final version of manuscript.

REFERENCES

Baker CA, Carlson BA. Short-term depression, temporal summation, and onset inhibition shape interval tuning in midbrain neurons. *J Neurosci* 34: 14272–14287, 2014.

Bauer M, von Helversen O. Separate localization of sound recognizing and sound producing neural mechanisms in a grasshopper. *J Comp Physiol A* 161: 95–101, 1987.

Boyan G. Common synaptic drive to segmentally homologous interneurons in the locust. *J Comp Neurol* 321: 544–554, 1992.

Clemens J, Kutzki O, Ronacher B, Schreiber S, Wohlgemuth S. Efficient transformation of an auditory population code in a small sensory system. *Proc Natl Acad Sci USA* 108: 13812–13817, 2011.

Clemens J, Wohlgemuth S, Ronacher B. Nonlinear computations underlying temporal and population sparseness in the auditory system of the grasshopper. *J Neurosci* 32: 10053–10062, 2012.

Dan Y, Poo M. Spike timing-dependent plasticity of neural circuits. *Neuron* 44: 23–30, 2004.

de Boer E. Auditory time constants: a paradox? In: *Time Resolution in Auditory Systems*, edited by Michelsen A. Berlin, Germany: Springer, 1985, p. 141–158.

Ehrlich D, Casseday JH, Covey E. Neural tuning to sound duration in the inferior colliculus of the big brown bat, *Eptesicus fuscus*. *J Neurophysiol* 77: 2360–2372, 1997.

Faure PA, Hoy RR. Neuroethology of the katydid T-cell. I. Tuning and responses to pure tones. *J Exp Biol* 203: 3225–3242, 2000.

Franz A, Ronacher B. Temperature dependence of temporal resolution in an insect nervous system. *J Comp Physiol A Neuroethol Sens Neural Behav Physiol* 188: 261–271, 2002.

Fortune ES, Rose GJ. Short-term synaptic plasticity as a temporal filter. *Trends Neurosci* 24: 381–385, 2001.

Garner WR. The effect of frequency spectrum on temporal integration of energy in the ear. *J Acoust Soc Am* 19: 808–815, 1947.

Gollisch T, Herz AV. Disentangling sub-millisecond processes within an auditory transduction chain. *PLoS Biol* 3: 144–154, 2005.

Gollisch T, Schütze H, Benda J, Herz AV. Energy integration describes sound-intensity coding in an insect auditory system. *J Neurosci* 22: 10434–10448, 2002.

Green DM. Temporal factors in psychoacoustics. In: *Time Resolution in Auditory Systems*, edited by Michelsen A. Berlin, Germany: Springer, 1985, p. 122–140.

Halex H, Kaiser W, Kalmring K. Projection areas and branching patterns of the tympanal receptor cells in migratory locusts, *Locusta migratoria* and *Schistocerca gregaria*. *Cell Tissue Res* 253: 517–528, 1988.

He J, Hashikawa T, Ojima H, Kinouchi Y. Temporal integration and duration tuning in the dorsal zone of cat auditory cortex. *J Neurosci* 17: 2615–2625, 1997.

Heil P. First-spike latency of auditory neurons revisited. *Curr Opin Neurobiol* 14: 461–467, 2004.

Heil P, Neubauer H. Temporal integration of sound pressure determines thresholds of auditory-nerve fibers. *J Neurosci* 21: 7404–7415, 2001.

Heil P, Neubauer H. A unifying basis of auditory thresholds based on temporal summation. *Proc Natl Acad Sci USA* 100: 6151–6156, 2003.

Heil P, Verhey JL, Zoefel B. Modelling detection thresholds for sounds repeated at different delays. *Hear Res* 296: 83–95, 2013.

Hennig RM, Heller KG, Clemens J. Time and timing in the acoustic recognition system of crickets. *Front Physiol* 5: 286 2014.

Henry KR. Enhancement of the cochlear nerve compound action potential: sharply defined frequency-intensity domains bordering the tuning curve. *Hear Res* 56: 239–245, 1991.

Hildebrandt KJ. Neural maps in insect versus vertebrate auditory systems. *Curr Opin Neurobiol* 24: 82–87, 2014.

Jacobs K, Otte B, Lakes-Harlan R. Tympanal receptor cells of *Schistocerca gregaria*: correlation of soma positions and dendrite attachment sites, central projections and physiologies. *J Exp Zool* 283: 270–285, 1999.

Jiang D, Palmer AR, Winter IM. Frequency extent of two-tone facilitation in onset units in the ventral cochlear nucleus. *J Neurophysiol* 75: 380–395, 1996.

Kastelein RA, Hoek L, de Jong CA, Wensveen PJ. The effect of signal duration on the underwater detection thresholds of a harbor porpoise (*Phocoena phocoena*) for single frequency-modulated tonal signals between 0.25 and 160 kHz. *J Acoust Soc Am* 128: 3211–3222, 2010.

Lütkenhöner B. Auditory signal detection appears to depend on temporal integration of subthreshold activity in auditory cortex. *Brain Res* 1385: 206–216, 2011.

Machens CK, Stemmler MB, Prinz P, Krahe R, Ronacher B, Herz AV. Representation of acoustic communication signals by insect auditory receptor neurons. *J Neurosci* 21: 3215–3227, 2001.

Marquart V. Local interneurons mediating excitation and inhibition onto ascending neurons in the auditory pathway of the grasshopper. *Naturwissenschaften* 72: 42–44, 1985.

Michelsen A. The physiology of the locust ear. I. Frequency sensitivity of single cells in the isolated ear. *Z Vergl Physiologie* 71: 49–62, 1971.

Nagel KI, Doupe AJ. Temporal processing and adaptation in the songbird auditory forebrain. *Neuron* 51: 845–859, 2006.

Neuhofer D, Wohlgemuth S, Stumpner A, Ronacher B. Evolutionarily conserved coding properties of auditory neurons across grasshopper species. *Proc R Soc B* 275: 1965–1974, 2008.

Okanoya K, Dooling RJ. Temporal integration in zebra finches (*Poephila guttata*). *J Acoust Soc Am* 87: 2782–2784, 1990.

Oswald AM, Schiff ML, Reyes AD. Synaptic mechanisms underlying auditory processing. *Curr Opin Neurobiol* 16: 371–376, 2006.

Pearson KG, Boyan GS, Bastiani M, Goodman CS. Heterogeneous properties of segmentally homologous interneurons in the ventral nerve cord of locusts. *J Comp Neurol* 233: 133–145, 1985.

Plomp R, Bouman MA. Relation between hearing threshold and duration for tone pulses. *J Acoust Soc Am* 31: 749–758, 1959.

Prinz P, Ronacher B. Temporal modulation transfer functions in auditory receptor fibres of the locust (*Locusta migratoria* L.). *J Comp Physiol A Neuroethol Sens Neural Behav Physiol* 188: 577–587, 2002.

Remme MW, Rinzel J. Role of active dendritic conductances in subthreshold input integration. *J Comput Neurosci* 31: 13–30, 2011.

Rokem A, Watzl S, Gollisch T, Stemmler M, Herz AV, Samengo I. Spike-timing precision underlies the coding efficiency of auditory receptor neurons. *J Neurophysiol* 95: 2541–2552, 2006.

Römer H. Die Informationsverarbeitung tympanaler Rezeptorelemente von *Locusta migratoria* (Acrididae, Orthoptera). *J Comp Physiol A* 109: 101–122, 1976.

Römer H, Marquart V. Morphology and physiology of auditory interneurons in the metathoracic ganglion of the locust. *J Comp Physiol A Neuroethol Sens Neural Behav Physiol* 155: 249–262, 1984.

Ronacher B. Processing of species-specific signals in the auditory pathway of grasshoppers. In: *Insect Hearing and Acoustic Communication*, edited by Hedwig B. Berlin, Germany: Springer, 2014, p. 185–204.

Ronacher B, Franz A, Wohlgemuth S, Hennig RM. Variability of spike trains and the processing of temporal patterns of acoustic signals - problems, constraints, and solutions. *J Comp Physiol A Neuroethol Sens Neural Behav Physiol* 190: 257–277, 2004.

Ronacher B, Hennig RM, Clemens J. Computational principles underlying recognition of acoustic signals in grasshoppers and crickets. *J Comp Physiol A Neuroethol Sens Neural Behav Physiol* 201: 61–71, 2015.

Ronacher B, Krahe R. Song recognition in the grasshopper *Chorthippus biguttulus* is not impaired by shortening song signals: implications for neuronal encoding. *J Comp Physiol A Neuroethol Sens Neural Behav Physiol* 183: 729–735, 1998.

Ronacher B, Krahe R. Temporal integration vs. parallel processing: coping with the variability of neuronal messages in directional hearing of insects. *Eur J Neurosci* 12: 2147–2156, 2000.

Ronacher B, von Helversen D, von Helversen O. Routes and stations in the processing of auditory directional information in the CNS of a grasshopper, as revealed by surgical experiments. *J Comp Physiol A* 158: 363–374, 1986.

Ronacher B, Wohlgemuth S, Vogel A, Krahe R. Discrimination of acoustic communication signals by grasshoppers (*Chorthippus biguttulus*): temporal resolution, temporal integration, and the impact of intrinsic noise. *J Comp Psychol* 122: 252–263, 2008.

Sabourin P, Gottlieb H, Pollack GS. Carrier-dependent temporal processing in an auditory interneuron. *J Acoust Soc Am* 123: 2910–2917, 2008.

Saija JD, Andringa TC, Bas¸kent D, Akyürek EG. Temporal integration of consecutive tones into synthetic vowels demonstrates perceptual assembly in audition. *J Exp Psychol Hum Percept Perform* 40: 857–869, 2014.

Schiolten P, Larsen ON, Michelsen A. Mechanical time resolution in some insect ears. *J Comp Physiol A* 143: 289–295, 1981.

Stange N, Ronacher B. Grasshopper calling songs convey information about condition and health of males. *J Comp Physiol A Neuroethol Sens Neural Behav Physiol* 198: 309–318, 2012.

Stumpner A, Ronacher B. Auditory interneurones in the metathoracic ganglion of the grasshopper (*Chorthippus biguttulus*). I. Morphological and physiological characterization. *J Exp Biol* 158: 391–410, 1991.

Stumpner A, Ronacher B, von Helversen O. Auditory interneurones in the metathoracic ganglion of the grasshopper (*Chorthippus biguttulus*). II. Processing of temporal patterns of the song of the male. *J Exp Biol* 158, 411–430, 1991.

Stumpner A, von Helversen D. Evolution and function of auditory systems in insects. *Naturwissenschaften* 88: 159–170, 2001.

Surlykke A, Bojesen O. Integration time for short broad band clicks in echolocating FM-bats (*Eptesicus fuscus*). *J Comp Physiol A* 178: 235–241, 1996.

Surlykke A, Larsen ON, Michelsen A. Temporal coding in the auditory receptor of the moth ear. *J Comp Physiol A* 162: 367–374, 1988.

Tougaard J. Energy detection and temporal integration in the noctuid A1 auditory receptor. *J Comp Physiol A* 178: 669–677, 1996.

Tougaard J. Detection of short pure-tone stimuli in the noctuid ear: what are temporal integration and integration time all about*? J Comp Physiol A* 183: 563–572, 1998.

Viemeister NF, Shivapuja BG, Recio A. Physiological correlates of temporal integration. In: *Auditory Physiology and Perception*, edited by Cazals Y, Demany L, Horner K. Oxford, UK: Pergamon, 1992, p. 323–329.

Viemeister NF, Wakefield GH. Temporal integration and multiple looks. *J Acoust Soc Am* 90: 858–865, 1991.

Vogel A, Hennig RM, Ronacher B. Increase of neuronal response variability at higher processing levels as revealed by simultaneous recordings. *J Neurophysiol* 93: 3548–3559, 2005.

Vogel A, Ronacher B. Neural correlations increase between consecutive processing levels in the auditory system of locusts. *J Neurophysiol* 97: 3376–3385, 2007.

von Helversen D. Gesang des Männchens und Lautschema des Weibchens bei der Feldheuschrecke *Chorthippus biguttulus* (Orthoptera, Acrididae). *J Comp Physiol* 81: 381–422, 1972.

Weschke G, Ronacher B. Influence of sound pressure level on the processing of amplitude modulations by auditory neurons of the locust. *J Comp Physiol A Neuroethol Sens Neural Behav Physiol* 194: 255–265, 2008.

Windmill JF, Bockenhauer S, Robert D. Time-resolved tympanal mechanics of the locust. *J R Soc Interface* 5: 1435–1443, 2008.

Wohlgemuth S, Vogel A, Ronacher B. Encoding of amplitude modulations by auditory neurons of the locust: influence of modulation frequency, rise time, and modulation depth. *J Comp Physiol A Neuroethol Sens Neural Behav Physiol* 197: 61–74, 2011.

Zucker RS, Regehr WG. Short-term synaptic plasticity. *Annu Rev Physiol* 64: 355–405. 2002.

Zwislocki J. Theory of temporal auditory summation. *J Acoust Soc Am* 32: 1046–1059, 1960.

Zwislocki J, Hellman RP, Verrillo RT. Threshold of audibility for short pulses. *J Acoust Soc Am* 34: 1648–1652, 1962.